Title

Regulation of LC3 lipidation by the autophagy-specific class III phosphatidylinositol-3 kinase complex

Journal

Molecular Biology of the Cell, 30(9)

ISSN

1059-1524

Authors

Brier, Livia W

Ge, Liang

Stjepanovic, Goran

et al.

Publication Date

2019-04-15

DOI

10.1091/mbc.e18-11-0743

Peer reviewed

Regulation of LC3 lipidation by the autophagy-specific class III phosphatidylinositol-3 kinase complex

Livia W. Brier[a,b], Liang Ge[a,b], Goran Stjepanovic[a,c,d], Ashley M. Thelen[a], James H. Hurley[a,c,d], and Randy Schekman[a,b,*]

[a]Department of Molecular and Cell Biology, [b]Howard Hughes Medical Institute, and [c]California Institute for Quantitative Biosciences, University of California, Berkeley, Berkeley, CA 94270; [d]Molecular Biophysics and Integrated Bioimaging Division, Lawrence Berkeley National Laboratory, Berkeley, CA 94720

ABSTRACT **Autophagy is a conserved eukaryotic pathway critical for cellular adaptation to changes in nutrition levels and stress. The class III phosphatidylinositol (PI)3-kinase complexes I and II (PI3KC3-C1 and -C2) are essential for autophagosome initiation and maturation, respectively, from highly curved vesicles. We used a cell-free reaction that reproduces a key autophagy initiation step, LC3 lipidation, as a biochemical readout to probe the role of autophagy-related gene (ATG)14, a PI3KC3-C1-specific subunit implicated in targeting the complex to autophagy initiation sites. We reconstituted LC3 lipidation with recombinant PI3KC3-C1, -C2, or various mutant derivatives added to extracts derived from a CRISPR/Cas9-generated ATG14-knockout cell line. Both complexes C1 and C2 require the C-terminal helix of VPS34 for activity on highly curved membranes. However, only complex C1 supports LC3 lipidation through the curvature-targeting amphipathic lipid packing sensor (ALPS) motif of ATG14. Furthermore, the ALPS motif and VPS34 catalytic activity are required for downstream recruitment of WD-repeat domain phosphoinositide-interacting protein (WIPI)2, a protein that binds phosphatidylinositol 3-phosphate and its product phosphatidylinositol 3, 5-bisphosphate, and a WIPI-binding protein, ATG2A, but do not affect membrane association of ATG3 and ATG16L1, enzymes contributing directly to LC3 lipidation. These data reveal the nuanced role of the ATG14 ALPS in membrane curvature sensing, suggesting that the ALPS has additional roles in supporting LC3 lipidation.**

Monitoring Editor
Gia Voeltz
University of Colorado, Boulder

Received: Dec 3, 2018
Revised: Feb 12, 2019
Accepted: Feb 20, 2019

This article was published online ahead of print in MBoC in Press (http://www.molbiolcell.org/cgi/doi/10.1091/mbc.E18-11-0743) on February 27, 2019.

*Address correspondence to: Randy Schekman (schekman@berkeley.edu).

Abbreviations used: ALPS, amphipathic lipid packing sensor; ATG, autophagy-related gene; BATS, Barkor autophagosome targeting sequence; ER, endoplasmic reticulum; ERGIC, ER-Golgi intermediate compartment; IB, immunoblot; KD, kinase deficient; KO, knockout; LUVs, large unilamellar vesicles; PC, phosphatidylcholine; PE, phosphatidylethanolamine; PI, phosphatidylinositol; PI3K, phosphatidylinositol 3-kinase; PI3KC3-C1, class III phosphatidylinositol 3-kinase complex I; PI3KC3-C2, class III phosphatidylinositol 3-kinase complex II; PS, phosphatidylserine; PtdIns3P, phosphatidylinositol 3-phosphate; PtdIns(3,5)P2, phosphatidylinositol 3,5-bisphosphate; RPN I, ribophorin I; SUVs, small unilamellar vesicles; VPS, vacuole protein sorting; WIPI, tryptophan-aspartic acid (WD)-repeat domain phosphoinositide-interacting proteins.

INTRODUCTION

Macroautophagy (hereafter referred to as autophagy) is essential for maintaining cellular homeostasis as it is activated by nutritional stress to induce bulk turnover of cytoplasmic contents (Mizushima *et al.*, 2008; Choi *et al.*, 2013; Mercer *et al.*, 2018). Upon activation, a cup-like structure called the phagophore forms and elongates, engulfing bulk cytoplasm or targeted cargo using membrane derived from cellular sources that have been identified as the endoplasmic reticulum (ER), ER-Golgi intermediate compartment (ERGIC), Golgi apparatus, recycling endosomes, mitochondria, plasma membrane, ER-mitochondria contact sites, or the dynamic autophagy-related gene (ATG)9 compartment (Ge *et al.*, 2014a; Mercer *et al.*, 2018). After the growing phagophore engulfs and seals cargo into a double membrane autophagosome, it travels to the lysosome into which it deposits its cargo for degradation (Rubinsztein *et al.*, 2012; Lamb *et al.*, 2013; Ge *et al.*, 2014a). Because it is a fundamental homeostasis control mechanism,

autophagy has been implicated in a variety of human disorders, yet the molecular mechanisms by which mammalian autophagy activation signals are translated into phagophore formation are still emerging.

More than two decades of research has identified and characterized the hierarchy of machinery that initiates and organizes autophagosome formation (Behrends *et al.*, 2010; Hurley and Schulman, 2014; Young and Hurley, 2017; Mercer *et al.*, 2018). Briefly, upon autophagy initiation, the ULK1 kinase complex is activated and translocates to the phagophore. This activated kinase complex then recruits ATG9, a multispanning transmembrane protein, and the class III phosphatidylinositol (PI)3-kinase complex I (PI3KC3-C1) that produces the signaling lipid, phosphatidylinositol 3-phosphate (PtdIns3P) to the phagophore membrane. Next, PtdIns3P can be converted to phosphatidylinositol 3, 5-bisphosphate (PtdIns[3,5]P2) by additional lipid kinase activity, and the two phospholipids can recruit effectors such as the double-FYVE containing protein 1, the tryptophan-aspartic acid (WD)-repeat domain phosphoinositide-interacting proteins (WIPI) family proteins and their binding partners, such as ATG2A, to the phagophore. Downstream of ULK1 and PI3KC3-C1 activity, two ubiquitin-like enzymatic cascades work to form the autophagic marker and cargo tether, LC3-II, by conjugating the cytosolic LC3-I protein to phosphatidylethanolamine (PE). The final LC3 lipidation reaction is orchestrated by ATG7, ATG3, and a complex consisting of ATG12-ATG5 and ATG16L1 serving as E1, E2, and E3-like enzymes, respectively, to form LC3-II by conjugating the cytosolic LC3-I protein to PE.

Successful autophagosome formation requires an orchestrated manipulation of highly curved membrane vesicles, tubes, and sheets. Because it is one of the first complexes recruited to the phagophore, creates an essential signaling lipid, PtdIns3P, and contains several domains that preferentially bind highly curved membranes (Fan *et al.*, 2011; Nguyen *et al.*, 2017; Young and Hurley, 2017), the autophagy-specific PI3KC3-C1 is a key regulator of autophagosome formation. However, the direct mechanism by which the complex and its product, PtdIns3P, orchestrate autophagosome formation by coordinating recruitment and activation of autophagic machinery on the phagophore membrane in vivo is unclear.

There are at least two forms of the PI3KC3 heterotetramer involved in distinct stages of mammalian autophagy (Itakura and Mizushima, 2009; Matsunaga *et al.*, 2009). Both contain the core machinery of vacuole protein sorting (VPS) 15, VPS34, and BECN1. Complex one (PI3KC3-C1), primarily involved in autophagosome formation, is defined by the presence of the autophagy-specific ATG14 (Itakura *et al.*, 2008; Sun *et al.*, 2008; Matsunaga *et al.*, 2009; Zhong *et al.*, 2009) and the metabolic switch, NRBF2 (Zhong *et al.*, 2014; Young *et al.*, 2016; Ma *et al.*, 2017). Complex two (PI3KC3-C2), which replaces ATG14 with UVRAG, is principally involved in later stages of autophagosome and endosome maturation (Itakura and Mizushima, 2009; Matsunaga *et al.*, 2009).

As an autophagy-specific factor of PI3KC3-C1, ATG14 is likely the key regulator of autophagy-induced translocation of this complex to the phagophore. Previous work has demonstrated that ATG14 contains an ATG14/Barkor autophagosome targeting sequence (BATS) domain that is required for recruiting the PI3KC3-C1 complex to the autophagosome membrane by sensing curvature in these membranes (Fan *et al.*, 2011; Wilz *et al.*, 2011; Hurley and Schulman, 2014). The BATS domain includes a predicted amphipathic lipid packing sensor (ALPS) motif on its extreme C-terminus (Drin *et al.*, 2007; Gautier *et al.*, 2008; Fan *et al.*, 2011; Wilz *et al.*, 2011). We predict that the ATG14 ALPS motif serves as a membrane curvature sensor responsible for targeting the PI3KC3-C1 complex to the highly curved phagophore membrane as the BATS domain membrane association capabilities are abolished when the bulky hydrophobic residues within the ALPS motif are mutated (Fan *et al.*, 2011).

Our group has established a cell-free reaction that faithfully reconstitutes LC3 lipidation and early stages of phagophore formation (Ge *et al.*, 2013). We adapted this assay to examine the PI3KC3-C1 complex by employing reconstitutions of CRISPR/Cas9-generated ATG14 knockout (KO) cytosolic fractions and purified recombinant PI3KC3-C1. We used this biochemical reconstitution assay to directly assess how the PI3KC3-C1, particularly its PI3K catalytic activity and membrane curvature sensing capabilities, regulate autophagy through LC3 lipidation and membrane association of autophagy machinery. We found that PI3KC3-C1 catalytic activity and the ATG14 ALPS domain were directly responsible for LC3 lipidation, the recruitment of WIPI2 and ATG2A, and PtdIns3P production. The PI3KC3-C2 complex by itself did not overcome ATG14 depletion. However, the membrane association of ULK1 complex components and critical LC3 lipidation machinery was not affected by defects in PI3KC3-C1 activity despite the requirement of this activity to promote the production of lipidated LC3-II.

RESULTS

ATG14 is required for LC3 lipidation

To probe the role of the PI3KC3-C1 in autophagy initiation, we adapted our previously established cell-free LC3 lipidation reaction that combines membrane fractions from ATG5 KO mouse embryonic fibroblast (MEF) cells, which cannot support LC3 lipidation, with cytosolic fractions from autophagy-induced cells (Ge *et al.*, 2013). After the addition of recombinant T7-LC3-I, GTP, and an ATP regeneration system, the resultant autophagy activity was observed by quantifying the conversion of precursor LC3-I to LC3-II product in the membrane fraction by SDS–PAGE and immunoblot (IB) (Supplemental Figure S1) (Ge *et al.*, 2013).

ATG14 is required for PI3KC3-C1 complex membrane targeting and autophagy initiation (Sun *et al.*, 2008; Matsunaga *et al.*, 2010; Fan *et al.*, 2011). Therefore, to directly study this complex in autophagy initiation, we focused on ATG14 activity by depleting it from cells. We used CRISPR/Cas9 (Cong *et al.*, 2013; Jinek *et al.*, 2013) to target the first exon of ATG14 in HEK293T cells creating an ATG14 KO cell line from which a cytosol fraction was isolated (Figure 1A and Supplemental Table S1). To remove active PI3KC3-C1 from the membrane fraction, we treated ATG5 KO MEF cells with the PI3K inhibitor, wortmannin (Blommaart *et al.*, 1997). Wortmannin-inactivated VPS34 is undetectable by IB in cellular membrane fractions of starved cells (Figure 1B). Wild-type cytosol combined with the wortmannin-treated membrane fraction supported LC3 lipidation (Figure 1C, lane 1). Conversely, lipidation efficiency with ATG14 KO cytosol dropped by more than 80% compared with wild-type cytosol (Figure 1C, lane 2).

To confirm that the decline in LC3-II production observed with ATG14 KO cytosol was specific, we complemented the reaction with purified recombinant PI3KC3-C1 (Figure 1D) (Baskaran *et al.*, 2014) at levels comparable to wild-type levels of VPS34 (Supplemental Figure S2). Recombinant PI3KC3-C1 stimulated and fully complemented LC3 lipidation in the ATG14-depleted system in a dose-dependent manner (Figure 1C). Lipidation complementation was a direct result of increased VPS34 activity as the addition of either wortmannin or a GST-FYVE peptide that binds and sequesters available PtdIns3P (Ridley *et al.*, 2001; Ge *et al.*, 2013) reduced lipidation levels to that observed without recombinant PI3KC3-C1 (Figure 1E).

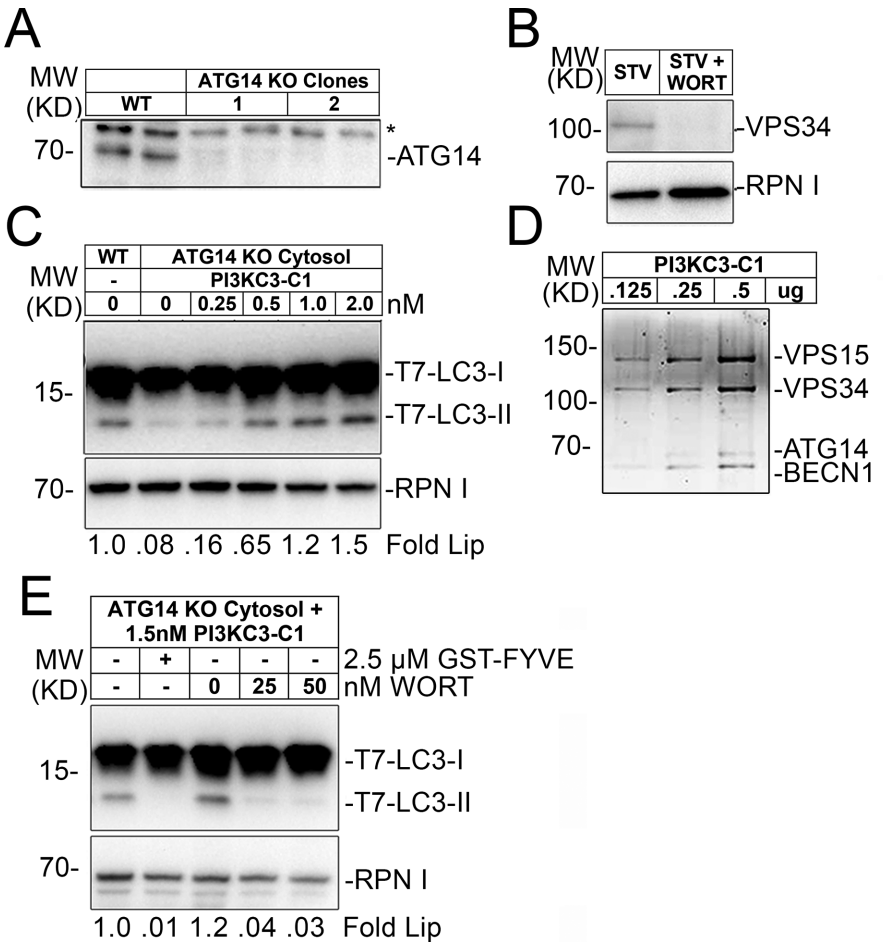

FIGURE 1: ATG14 KO cytosol does not support cell-free lipidation of LC3. (A) IB of cell lysate from two CRISPR/Cas9-generated ATG14 KO HEK 293T clones. Clone 2 was used in this study. *Nonspecific band. (B) ATG5 KO MEFs starved in EBSS for 1 h with 20 nM wortmannin (Wort) where indicated. Membrane fractions were harvested and evaluated by SDS–PAGE and IB. (C) LC3 lipidation reaction performed as detailed in (Supplemental Figure S1). Cytosol type and PI3KC3-C1 concentrations are noted. (RPN I), ribophorin I loading control. Fold lipidation levels are LC3-II/LC3-I levels in relation to lane 1. (D) A titration of recombinantly expressed and purified PI3KC3-C1 complex visualized with SYPRO Red. (E) Lipidation reaction performed and analyzed as in C with indicated reagents.

PI3KC3-C1 activity is necessary for LC3 lipidation

Several studies using wortmannin or other VPS34 inhibitors have uncovered that its lipid kinase activity is required for LC3 lipidation early in the autophagic pathway (Miller *et al.*, 2010; Ge *et al.*, 2013, 2014b; Ronan *et al.*, 2014; Pasquier *et al.*, 2015). To directly understand the role of VPS34 activity in LC3 lipidation, we created and purified a kinase-deficient (KD) PI3KC3-C1 by mutating D743A and N748I in the magnesium-binding pocket of the VPS34 catalytic domain (Supplemental Figure S3A) (Miller *et al.*, 2010). The KD mutant has no catalytic activity compared with wild-type PI3KC3-C1 (Figure 2A) and did not stimulate LC3 lipidation in an ATG14-depleted system (Figure 2B). Therefore, VPS34 kinase activity in the PI3KC3-C1 complex is necessary for LC3-II lipidation.

In addition to confirming a direct requirement for VPS34 activity in LC3 lipidation, we probed the role of PtdIns3P in the ATG14-depleted system. We incorporated exogenous PtdIns3P within small unilamellar vesicles (SUVs) into the ATG5 KO membrane fraction and then assayed lipidation activity. Exogenous PtdIns3P stimulated LC3 lipidation with both wild-type and ATG14 KO cytosol (Figure 2C). Lipidation defects in the ATG14-depleted system were fully complemented by the addition of 100 μM PtdIns3P. Consequently, PtdIns3P production is necessary and sufficient in fulfilling the role of ATG14 in stimulating LC3 lipidation in the reconstituted autophagy system.

PI3KC3-C2 does not complement ATG14-depletion defects

There are two PI3KC3 subcomplexes in mammalian cells: C1 regulates autophagy initiation and contains ATG14; C2 is primarily involved in late endosome and autophagosome maturation and contains UVRAG in the active complex (Liang *et al.*, 2008; Itakura and Mizushima, 2009; Zhong *et al.*, 2009; Kim *et al.*, 2013). We also purified recombinant PI3KC3-C2 (Supplemental Figure S3B) to probe its ability to stimulate LC3 lipidation and complement the defect associated with ATG14 depletion. First, we tested the relative catalytic activity of these two complexes based on membrane curvature using either large unilamellar vesicles (LUVs) or highly curved SUVs incorporated with the PtdIns3P precursor, PI. We found that C2 was 50% less active than C1 on SUVs, suggesting that C1 contains an additional factor that increased its activity on highly curved membranes (Figure 2D). We generated SUVs and LUVs and found that the catalytic activity of C1 and C2 was highly dependent on membrane curvature (Figure 2D). In contrast to a finding in a previous report (Rostislavleva *et al.*, 2015), the activity of both complexes decreased as vesicle diameter increased. We then compared the LC3 lipidation activity of these complexes and found that C1 robustly stimulates LC3 lipidation in a dose-dependent manner in incubations containing wild-type cytosol, whereas C2 does not (Figure 2, E and F). Additionally, C2 only modestly stimulates LC3 lipidation in a dose-dependent manner compared with C1 in reactions containing ATG14-KO cytosol (Figure 2, G and H). Thus, although the kinase complexes contain the same core machinery, the limited catalytic activity of PI3KC3-C2 on small vesicles cannot replace the C1 complex in stimulating lipidation of LC3, possibly due to a failure to target the C2 enzyme to a highly curved early autophagosome membrane template.

The ATG14 ALPS is critical for PI3KC3-C1 membrane targeting

ATG14 is responsible for targeting the PI3KC3-C1 to the autophagic membrane through its BATS domain (Fan *et al.*, 2011). The BATS domain preferentially binds highly curved membrane and encompasses a predicted ALPS motif (Gautier *et al.*, 2008; Antonny, 2011; Fan *et al.*, 2011; Wilz *et al.*, 2011). ALPS motifs are short 20–40 amino acid–long peptides that sense membrane curvature by inserting an alpha helix into lipid-packing defects inherent in highly curved membrane bilayers (Antonny, 2011).

We designed a PI3KC3-C1 mutant lacking the final 25 residues of ATG14 encompassing the ALPS motif (ΔALPS) (Figure 3A and

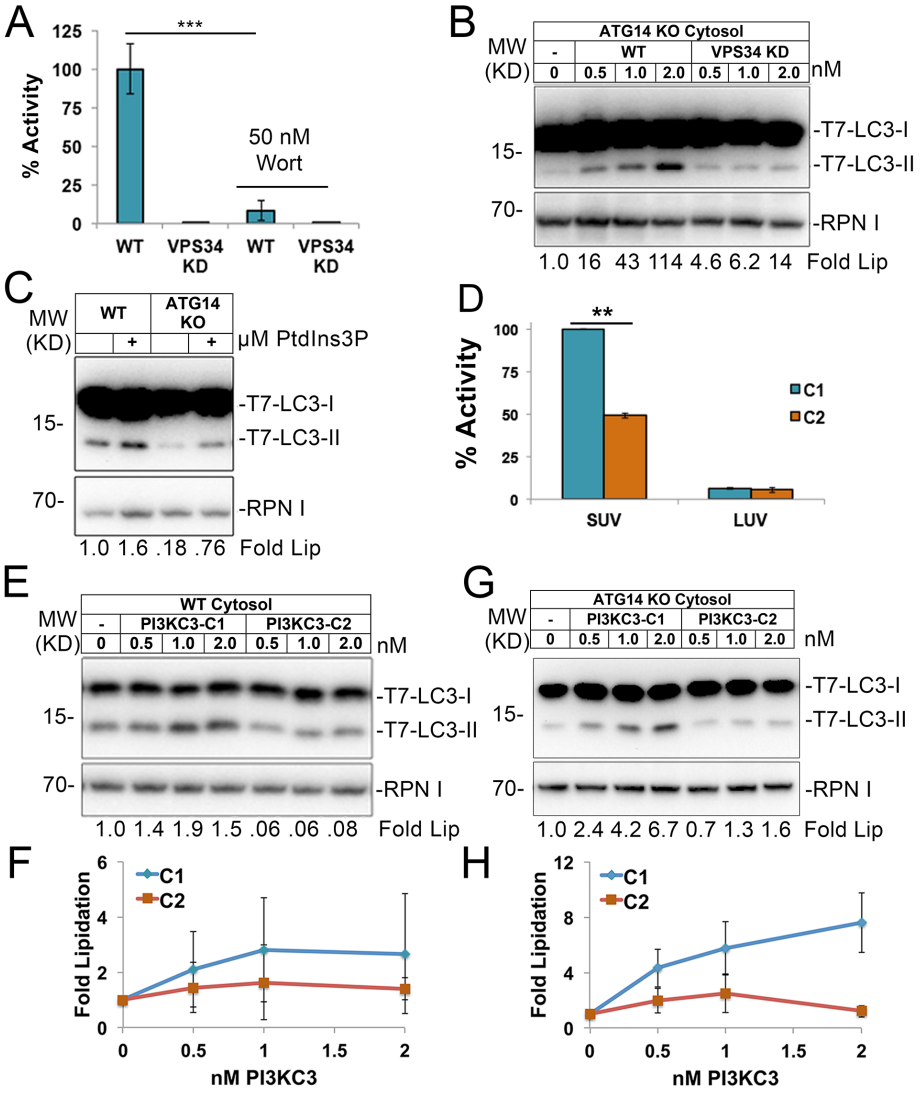

FIGURE 2: KD PI3KC3-C1 and PI3KC3-C2 do not complement ATG14 KO cytosol. (A) Mean percentage of kinase activity of PI3KC3-C1 complexes on PI/PS SUVs and 50 nM wortmannin where indicated using an ADP-GLO kinase assay (Baskaran *et al.*, 2014). $n = 3$. Error bars represent SD. ***$p < 0.001$. (B) LC3 lipidation reaction using a titration of wild-type or KD PI3KC3-C1 complexes. (C) Lipidation reaction performed with PtdIns3P incorporated membrane and analyzed as in B. (D) Mean percentage of kinase activity of indicated PI3KC3 complexes after thin-layer chromatography of radiolabeled PI(3)P generated from PI and [γ-32 P] ATP. Error bars represent SD. **$p < 0.01$. (E–H) LC3 lipidation reaction using equivalent concentrations of PI3KC3-C1 or -C2 complexes with either (E, F) wild-type or (G, H) ATG14 KO cytosol and analyzed as in B. (F, H) Average fold lipidation levels. Error bars represent SEM of $n = 6$.

Supplemental Figure S3C). An ALPS motif deletion decreased PI3KC3-C1 activity on SUVs by ~40% (Figure 3B), comparable to PI3KC3-C2 activity (Figure 2D). Thus, the ALPS motif provides additional highly curved membrane-targeting capabilities and increases C1 PI3K activity on these membranes. To assess any ΔALPS PI3KC3-C1 mutant complex membrane-association defects, we used a buoyant density flotation separation of incubations containing recombinant protein complexes mixed with the ATG5 KO membrane fraction used in LC3 lipidation reactions (Figure 3C). All wild-type PI3KC3-C1 subunits were present in the top membrane-bound fraction (Figure 3D). No components of the PI3KC3-C1 complex could be detected by IB of the buoyant membranes from incubations containing the ΔALPS PI3KC3-C1 mutant. Therefore, the ALPS motif is responsible for targeting a stable PI3KC3-C1 to the early autophagic membrane.

We then tested the LC3 lipidation activity of the ΔALPS PI3KC3-C1 mutant and found that it did not complement ATG14-depleted cytosol defects (Figure 3E). Therefore, although the ΔALPS PI3KC3-C1 mutant retained half of wild-type catalytic activity, it neither bound to membranes nor stimulated LC3 lipidation.

PI3KC3-C1 activity is required for WIPI2 and ATG2A membrane association

Imaging studies have uncovered that PI3K activity is required for stable phagophore localization of upstream autophagy machinery, such as the ULK1 kinase complex, and also downstream machinery, such as the LC3 lipidation machinery DFCP1, WIPI2, and ATG2A (Mizushima *et al.*, 2001; Axe *et al.*, 2008; Itakura and Mizushima, 2010; Koyama-Honda *et al.*, 2013; Kishi-Itakura *et al.*, 2014). However, because only WIPI proteins and DFCP1 contain a known PtdIns3P effector, the mechanism by which the PI3KC3-C1 regulates association of other factors and subsequent autophagy activity is unknown.

We isolated membrane fractions from our cell-free reaction to directly assess how the PI3KC3-C1 regulates the membrane association of the autophagy machinery. First, we treated the reactions with wortmannin to probe how membrane association differed after chemical PI3KC3-C1 inhibition. Wortmannin treatment drastically depleted membrane association of the PtdIns3P effector, WIPI2, and ATG2A, which binds another PtdIns3P effector, WIPI4 (Bakula *et al.*, 2017) (Figure 4, A and B). In contrast, although LC3 lipidation was inhibited by wortmannin, there were no significant changes in the membrane association of the lipidation components, ATG3 and ATG16L1, or of subunits of the ULK1 complex, FIP200 and ATG13 (Figure 4, A and B).

We next tested how ATG14 depletion and complementation affected the membrane association of components of the autophagy machinery. WIPI2 and ATG2A membrane association increased at least threefold in incubations containing a concentration of PI3KC3-C1 that complemented ATG14-depletion defects in the lipidation reaction (Figure 4, C and D). Although PI3KC3-C1 complementation stimulated LC3 lipidation activity, it did not significantly alter the membrane association of ATG16L1 and ATG3 or FIP200 and ATG13 (Figure 4, C and D).

PI3KC3-C2 and PI3KC3-C1 mutants lacking VPS34 catalytic activity or the ALPS motif did not complement ATG14-depletion lipidation defects (Figures 2 and 3). To determine whether these lipidation defects are a result of aberrant autophagy machinery membrane association, we examined their effect in the membrane

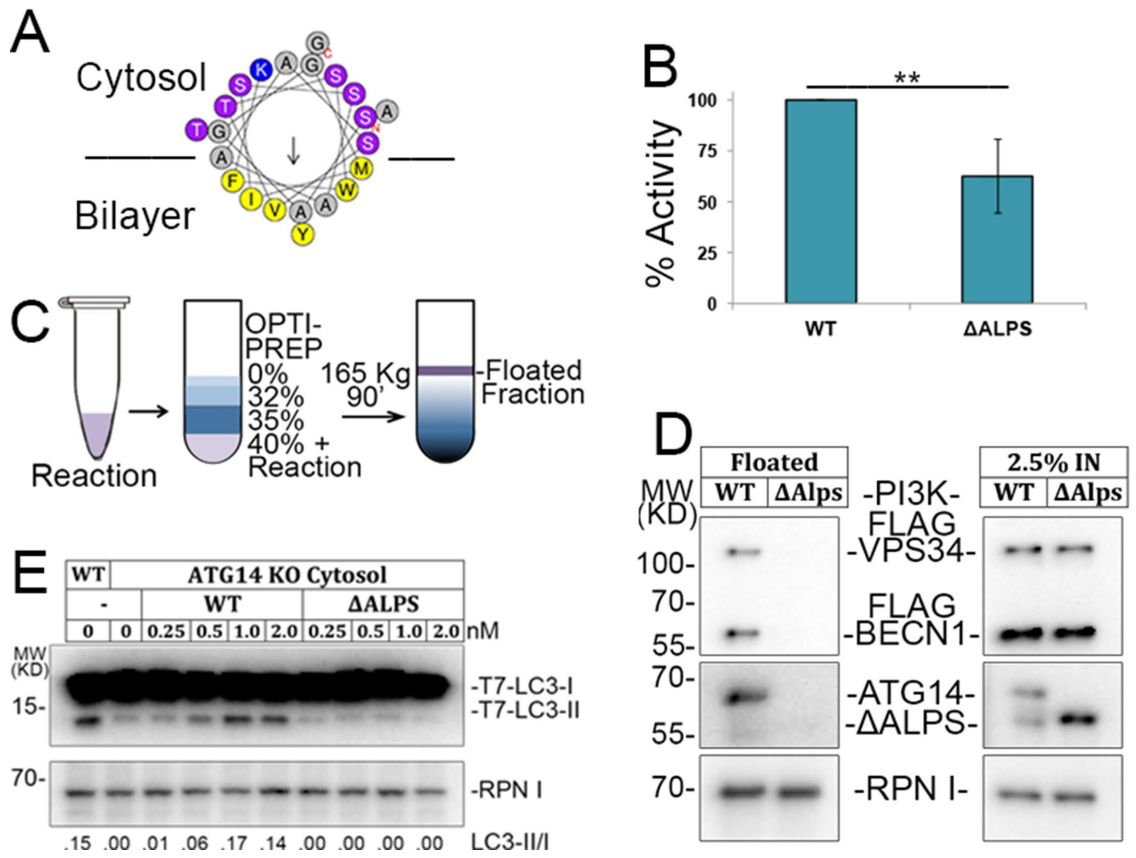

FIGURE 3: ΔALPS PI3KC3-C1 does not complement ATG14-KO cytosol. (A) Helical structure of the predicted ALPS motif of ATG14 analyzed using HELIQUEST (heliquest.ipmc.cnrs.fr) (Gautier *et al.*, 2008). (B) Percentage kinase activity of PI3KC3-C1 complexes on PI/PS SUVs and using an ADP-GLO kinase assay, $n = 4$. Error Bars represent SD, $^{**}p < 0.01$. (C) Schematic of a buoyant density membrane flotation assay. The reaction is mixed with a 50% OptiPrep solution to a final concentration of 40%. Then, 35%, 32%, and 0% OptiPrep solutions are layered above. After centrifugation for 90 min at 165,000 × *g*, the top fractions containing low-density samples with visible membrane are removed and evaluated by IB. (D) The ΔALPS PI3KC3-C1 mutant does not associate with lipidation reaction membrane. Wild-type and ΔALPS PI3KC3-C1 were combined with the ATG5 KO membrane fraction to a final concentration of 10 nM PI3KC3-C1 with a 1X ATP regeneration system and 0.15 mM GTP. Samples were incubated at for 60 min at 30°C and then subjected to an OptiPrep gradient centrifugation. The top floated fraction (90 µl) was removed and subjected to IB. (E) LC3 lipidation reaction using a titration of equivalent concentrations of wild-type or ΔALPS PI3KC3-C1 mutant.

recruitment assay. First, we tested the differences in C1 and C2 and found that C2 did not stimulate WIPI2 and ATG2A membrane association in an ATG14-depleted reaction (Figure 5, A and B), suggesting that PI3KC3-C2 failed to produce PtdIns3P in a location competent to recruit WIPI2 or ATG2A and to stimulate autophagosome formation.

We then complemented the ATG14-depleted reconstitution with wild-type, ΔALPS, and KD PI3KC3-C1 and found that only the wild-type PI3KC3-C1 stimulated WIPI2 and ATG2A membrane association (Figure 5, C and D). In contrast, ATG3 and ATG16L1 membrane association did not significantly change upon the addition of wild-type or mutant PI3KC3-C1 complexes, even though they displayed distinct defects of lipidation activity.

The ΔALPS mutant retained roughly 60% of wild-type kinase activity, enough to permit a test of the role for ALPS in PtdIns3P production. We assessed the production of PtdIns3P in the lipidation reaction by detecting the association of GST-FYVE peptide on membranes isolated from the reconstitution by buoyant density flotation. Changes in both GST-FYVE and WIPI2 membrane association may be used as reporters for the production of overall and autophagy-specific PtdIns3P, respectively. The addition of wild-type PI3KC3-C1 increased both GST-FYVE and WIPI2 membrane association, indicating an increase in PtdIns3P production (Figure 5E). The ΔALPS PI3KC3-C1 mutant did not stimulate WIPI2 or GST-FYVE association; therefore deleting the ATG14 ALPS motif abolished PI3KC3-C1 catalytic activity on isolated membranes.

DISCUSSION

In this study, we employed a biochemical approach to assess the roles that PI3KC3-C1 catalytic activity and the ability to associate with highly curved membranes have in autophagy factor membrane association and LC3 lipidation activity. We confirm through the use of a cell-free assay that PI3KC3-C1 activity and PtdIns3P production are necessary for LC3 lipidation. In addition, we uncovered that the ALPS motif of ATG14 is directly required for LC3 lipidation, PtdIns3P production, and the association of WIPI2 and ATG2A with

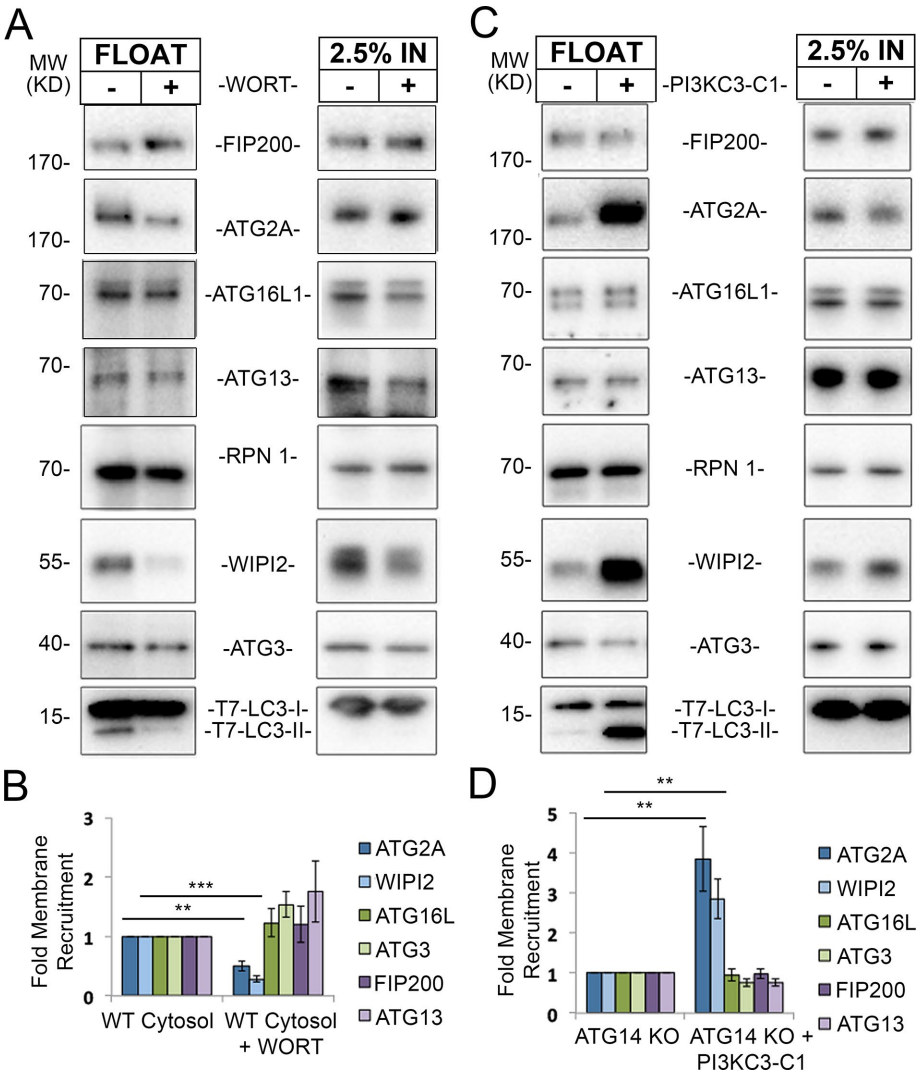

FIGURE 4: WIPI2 and ATG2A membrane association, not lipidation machinery, dependent on PI3KC3-C1 activity. (A) Membrane-buoyant density flotation performed using wild-type cytosol and 20 nM wortmannin where noted. After centrifugation, the top fraction (90 µl) containing the most buoyant membrane was collected and both input and floated fractions were analyzed by IB. (B) Quantification of experiments conducted in A. Fold membrane recruitment was determined by densitometry analysis of top and input bands normalized to RPN I loading control. $n = 4$, $^{***}p < 0.001$. (C) Reaction performed as in A except with ATG14 KO cytosol and 1 nM of wild-type PI3KC3-C1. (D) Quantification of experiments conducted in C. $n = 6$, $^{**}p < 0.01$.

membranes. The PI3KC3-C1 contains additional membrane association factors, such as a lipid anchor on VPS15 and the VPS34 C-terminal helix, which are also required for catalytic activity (Miller *et al.*, 2010). Therefore, the ALPS motif is likely critical for targeting the PI3KC3-C1 to the appropriate membrane microenvironment for phagophore expansion and elongation, such as the highly curved, PtdIns3P-enriched tips of the growing phagophore, where imaging studies have localized the PI3KC3-C1 complex in *Saccharomyces cerevisiae* (Obara *et al.*, 2008; Suzuki *et al.*, 2013) or the tubular structure of the ERGIC or ER-exit sites where PI3K activity is required for producing small autophagic precursor vesicles (Graef *et al.*, 2013; Ge *et al.*, 2014b).

Studies have suggested that PI3KC3-C2 is required for maturation and sorting of autophagosomes and endosomes as they are trafficked to the lysosome (Liang *et al.*, 2008; Itakura and Mizushima, 2009; Kim *et al.*, 2015). Others have demonstrated that the PI3KC3-C2, in association with another factor, Bif-1, is also localized to the phagophore and participates in autophagy initiation and ATG9 trafficking (Takahashi *et al.*, 2007, 2011; He *et al.*, 2013). Using our reconstituted autophagy initiation reaction, we find that the PI3KC3-C2 cannot stimulate LC3 lipidation under wild-type conditions or complement cytosol depleted of PI3KC3-C1. Although our recombinant PI3KC3-C2 does not contain Bif-1, this regulatory subunit of the C2 complex is present in a crude cytosol fraction but does not activate recombinant C2 complex mixed with cytosol in our cell-free reaction. Consequently, our evidence suggests that PI3KC3-C1 and C2 have clear functional differences in autophagy dictated by ATG14.

These data reveal the mechanism behind the important division of labor between two PI3KC3 complexes. Both C1 and C2 complexes have a preference for curved membranes; however, the preference of C1 is more pronounced as a result of the ALPS motif. Deletion of the ALPS motif reduces, but does not eliminate, activity on highly curved vesicles, yet it completely abrogates the ability of PI3KC3-C1 to support LC3 lipidation. Thus, the ALPS motif is likely to have additional functions beyond supporting high curvature binding.

WIPI2 and ATG2A membrane association is directly related to VPS34 kinase activity either by binding PtdIns3P or as a precursor for PtdIns(3,5)P2 production (Proikas-Cezanne *et al.*, 2004; Polson *et al.*, 2010; Velikkakath *et al.*, 2012). Therefore, as this study and others have demonstrated the importance of VPS34 activity for LC3 lipidation, it is likely that either WIPI family proteins or ATG2A regulates the lipidation machinery. Studies have suggested that WIPI2 and ATG2A (and their representative homologues in *S. cerevisiae*) do not directly affect LC3 lipidation to the same extent as other components of the autophagic machinery (Proikas-Cezanne *et al.*, 2004; Suzuki *et al.*, 2007; Polson *et al.*, 2010; Mauthe *et al.*, 2011; Velikkakath *et al.*, 2012). However, other studies have demonstrated that FIP200 and WIPI2 bind ATG16L1 isoforms and that this interaction and subsequent membrane association is responsible for ATG16L1-dependent lipidation of LC3 (Gammoh *et al.*, 2012; Nishimura *et al.*, 2013; Dooley *et al.*, 2014). In this study, we found that membrane association capabilities of LC3 lipidation machinery components ATG3 and ATG16L1, which have been shown to dictate the site of LC3 lipidation (Fujita *et al.*, 2008; Nath *et al.*, 2014), are not regulated by PI3KC3-C1 activity. However, as our study uses a cell-free approach to directly assess differences in membrane association, these distinctions in the role of FIP200 and WIPI2 in ATG16L1 recruitment may be a result of the sensitivity of different technical approaches.

WIPI2 and ATG2A are the only critical components of autophagy initiation machinery outside of the PI3KC3-C1 that change

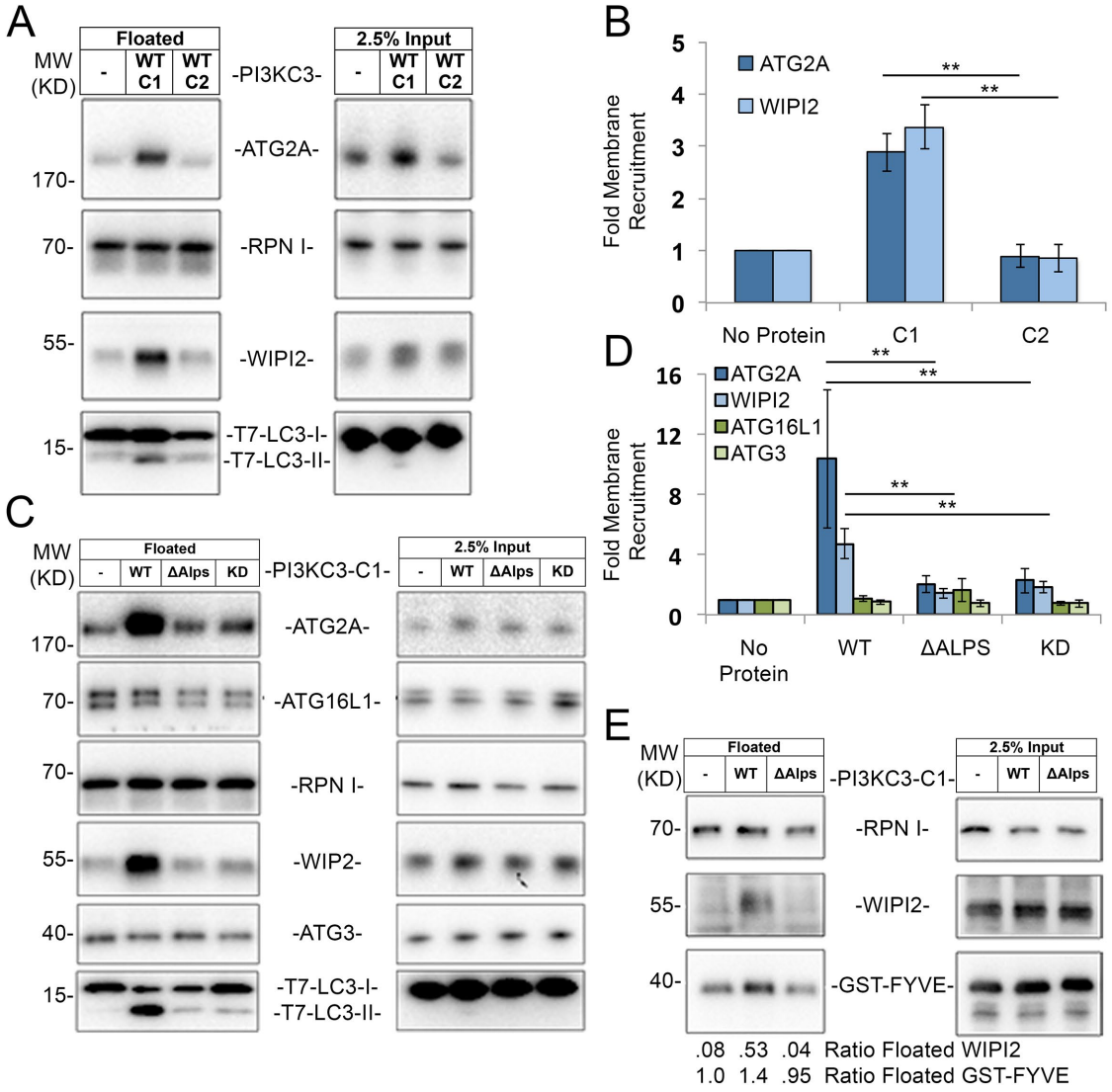

FIGURE 5: Only wild-type PI3KC3-C1 can produce PtdIns3P and stimulate WIPI2 and ATG2A recruitment in an ATG14-depleted system. (A) Membrane-buoyant density flotation performed with ATG14 KO cytosol and complemented with 1 nM of noted PI3KC3 complex. (B) Quantification of A. $n = 4$, $^{**}p < 0.01$. (C) Experiment performed as in A with ΔALPS and KD mutants. (D) Quantification of C, $n = 5$, $^{**}p < 0.01$. (E) Membrane-buoyant density flotation performed as in A but after the lipidation reaction, GST-FYVE peptide was added at 0.08 mg/ml and incubated for an additional 1 h at 30°C before density gradient sedimentation.

membrane association in correlation with lipidation activity in our recombinant reconstitution. However, either PtdIns3P concentrations higher than that necessary to stimulate LC3 lipidation may be required to stimulate this association, or additional lipid kinase activity may be required to produce PtdIns(3,5)P2 from PtdIns3P for robust membrane recruitment, as we could not reconstitute WIPI2 or ATG2A association with membranes in incubations containing exogenous PtdIns3P (unpublished data). Because the PI3KC3-C1 is required to produce small lipidation-competent vesicles and wortmannin-treated cells do not form a phagophore (Ge *et al.*, 2014b; Kishi-Itakura *et al.*, 2014), PI3KC3-C1 activity may indirectly stimulate LC3 lipidation by elongating the phagophore that can then support LC3 lipidation. Phagophore elongation and closure may be dependent on ATG2A, as cells lacking this factor accumulate LC3-II and form large LC3 positive puncta (Kishi-Itakura *et al.*, 2014) with autophagic cargo accessible to exogenous protease attack (Velikkakath *et al.*, 2012; Kishi-Itakura *et al.*, 2014; Zhang *et al.*, 2015). More studies are necessary to uncover this intriguing relationship among PI3KC3-C1 activity, WIPI2 and ATG2A membrane association, phagophore elongation, and LC3 lipidation.

Our study suggests a direct relationship among PI3KC3-C1 catalytic activity, LC3 lipidation, and autophagy activity. However, although PI3KC3-C1 activity regulates WIPI2 and ATG2A membrane association and LC3 lipidation, it does not directly regulate membrane association of components of the lipidation machinery. Therefore, the mechanism by which PtdIns3P production stimulates LC3 lipidation activity remains unknown. As the PI3KC3-C1 is a critical regulator of an important cellular homeostasis pathway, a more detailed understanding of its role in autophagy initiation may be critical in an effort to control autophagy for therapeutic purposes, particularly because highly specific VPS34 inhibitors fail to discriminate kinase activities of the C1 and C2 enzymes (Ronan *et al.*, 2014; Pasquier *et al.*, 2015). Here, we report that deleting a 25-residue-long membrane-targeting motif on ATG14 completely abolishes all

PI3KC3-C1 activity, thereby suggesting a potential target to control PI3K activity in the initiation of autophagy.

MATERIALS AND METHODS

Cytosol preparation

Cytosol fractions prepared from HEK 293T cells was conducted as previously described (Ge *et al.*, 2013) with adaptations. Confluent cells in 15-cm-diameter culture dishes were starved in 15 ml Earle's balanced saline solution (EBSS) for 1 h. After clarification by sedimentation 3 × 60 min at 165,000 × *g*, 4°C, the supernatant cytosol concentration was determined using protein-assay dye reagent (Bio-Rad, Hercules, CA). Samples were snap-frozen, stored at –80°C, and subjected to no more than one freeze–thaw cycle.

Membrane preparation

Membrane preparations from ATG5 KO cells were isolated as described in Ge *et al.* (2013) with adaptations to deplete PI3KC3-C1. ATG5 KO MEFS were grown to confluency in 15-cm-diameter culture dishes and washed 1× with sterile phosphate-buffered saline (PBS). Cells were then starved for 1 h in 15 ml EBSS with 20 nM wortmannin, collected, and lysed in 2.7× cell pellet volume of membrane lysis buffer (20 mM HEPES, pH 7.2, 1.0 mM EDTA, 250 mM sorbitol, 0.3 mM dithiothreitol [DTT], 1× Roche Protease Inhibitor Tablet, 1× Roche Phosphatase Inhibitor Tablet) by passing through a 22-G needle to achieve ~85% lysis, as assessed by trypan blue staining. To reduce lipid loss, all membrane was handled using low-retention pipette tips (Axygen). Cellular debris was sedimented by centrifugation for 10 min at 3000 × *g*, 4°C. After reserving the supernatant fraction, the pellet was washed and sedimented one more time. The two supernatant fractions were combined and the membrane fraction was isolated by sedimentation for 30 min at 25,000 × *g*, 4°C. The pellet was gently resuspended and washed one time in B88 lysis buffer (20 mM HEPES, pH 7.2, 250 mM sorbitol, 150 mM potassium acetate, 5 mM magnesium acetate, 0.3 mM DTT, 1× Roche Protease Inhibitor Tablet, 1× Roche Phosphatase inhibitor Tablet). Phosphatidylcholine (PC) concentration was used as a readout for overall lipid concentration and determined using the PC assay described in Ge *et al.* (2011). Membrane fractions were stored at 4°C and used within 24 h of preparation.

LC3-II lipidation reaction

The LC3-II lipidation reaction was adapted from Ge *et al.* (2013). For each lipidation reaction, a final concentration of 2.4 mg protein/ml cytosol, 0.1 mg/ml (PC content final concentration) of ATG5 KO membrane, ATP regeneration system (40 mM creatine phosphate, 0.2 mg/ml creatine phosphokinase, and 1 mM ATP), 0.15 mM GTP, and 10.0 µg protein/ml 3× T7-LC3 was diluted to a final volume of 18 µl in B88 lysis buffer. In experiments containing recombinant PI3KC3, we first diluted protein stocks to equivalent concentrations in PI3K freezing buffer (20 mM Tris–HCl, pH 8.0, 200 mM NaCl, 2 mM $MgCl_2$, and 1 mM TCEP, 10% vol/vol glycerol) and diluted to 12.5 nM in B88 buffer.

Samples were briefly agitated in a vortex mixer, centrifuged for 3 s at 10,000 × *g* to collect droplets and incubated for 70 min at 30°C. Membranes were then sedimented for 15 min at 20,000 × *g*, 4°C. The supernatant fraction was isolated and the pellet was resuspended in 35 µl of 1× SDS buffer (4 × SDS buffer diluted in PBS) by shaking for 5 min in a bead beater. Samples were prepared for SDS–PAGE by heating for 10 min at 65°C. LC3-II turnover was visualized by SDS–PAGE and IB using an 8–16% Criterion Tris–HCl Gel (3450039; Bio-Rad). Ratios of LC3-II over LC3-I were quantitated using ImageJ band analysis for densitometry.

PtdIns3P incorporated LC3-II lipidation reaction

To prepare liposomes, we dried 40 µl of a 1.0 mg/ml stock of 18:0 PtdIns3P (Avanti Polar Lipids) in chloroform overnight under a vacuum. The lipid was resuspended in 160 µl B88 by rotating for 1 h at 25°C. After resuspension, liposomes were extruded through a B88 equilibrated 100 nM Whatman Nucleopore Track Etch Membrane filter (Sigma) 30×. Lipids were then added to a mix of 0.1 mg/ml (PC content final concentration) of ATG5 KO membrane, ATP regeneration system, and 0.15 mM GTP and incubated for 1 h at 30°C.

After PtdIns3P incorporation, 2.4 mg/ml cytosol and 0.1 mg/ml 3× T7-LC3 were added to the membrane mixture to a final volume of 18 µl and incubated for 70 min at 30°C. Lipidation reaction samples were prepared and analyzed as described above.

ADP-Glo kinase assay

The ADP-Glo kinase assay (Promega, Madison, WI) protocol was adapted from previous protocols (Baskaran *et al.*, 2014) and performed in 96-well PS F-Bottom white plates (Greiner Bio-One, Frickenhausen, Germany). The 25-µl reaction consisted of 20 µl of 125 µM PI: phosphatidylserine (PS) (Avanti Polar Lipids, Alabaster, AL) SUVs in PI/PS buffer (50 mM HEPES, pH 7.0, 50 mM $MnCl_2$, 0.5 mM TCEP), and 2.5 µl of 100 nM recombinant PI3KC3 in PI3K freezing buffer and was initiated by adding 2.5 µl of 500 mM ATP. After incubation for 1 h at 37°C, the reaction was stopped by the addition of 25 µl ADP-Glo Reagent supplemented with 10 mM $MgCl_2$ for 40 min at 25°C. Then, 50 µl of Kinase Detection Reagent was added to wells and incubated for 30 min at 25°C. Luminescence was measured using an Infinite M1000 system (Tecan, Research Triangle Park, NC) with a 1000-ms integration time.

Buoyant density membrane recruitment assay

Membrane recruitment assays were conducted using a 48-µl LC3-II lipidation reaction from which 2.5% input samples were taken after incubation at 30°C. Samples were gently mixed with 50% OptiPrep in B88 to a final concentration of 40% Opti Prep in 200 µl. Layers of 130 µl of 35%, 120 µl of 32%, and 20 µl of 0% Opti Prep in B88 were added above the sample. Density gradients were centrifuged in a swinging bucket TLS-55 rotor (Beckman Coulter, Pasadena, CA) for 90 min at 165,000 × *g*, 4°C with reduced braking. Fractions (90 µl) were removed by pipette from the top. Samples were mixed with 4× SDS and prepared for SDS–PAGE and IB. Densitometry was calculated using ImageJ band analysis.

Statistical analysis

Unless noted, data are presented as the mean ± SEM and are representative of experiments conducted in triplicate at minimum. Two-tailed Student's *t* tests were conducted when indicated.

ACKNOWLEDGMENTS

This article is part of Livia Wilz Brier's doctoral dissertation at University of California, Berkeley, titled "Regulation of Autophagosome Biogenesis by the Autophagy Specific Class III Phosphatidyl Inostitol-3 Kinase Complex" that has been published online. We thank Qing Zhong, Nicholas Ktistakis, Noboru Mizushima, Masaaki Komatsu, David King, Kundu Mondira, Eisaku Hokazono, and Jennifer Lippincott-Schwartz for reagents and Bob Lesch, Jeremy Thorner, J. Christopher Anderson, Roberto Zoncu, Ann Fisher, Allison Killilea, and all members of the Schekman and Hurley labs (University of California, Berkeley) for technical assistance and helpful advice on the study. L.B. was supported by funds from the Howard Hughes Medical Institute (HHMI). L.G. was supported by a fellowship from the Human Frontier Science Program (HFSP) and

the Jane Coffin Childs Fund (JCCF). Work in the Hurley lab was supported by National Institutes of Health Grant GM-111730. R.S. is an Investigator of the HHMI and a Senior Fellow of the University of California, Berkeley Miller Institute.

REFERENCES

Antonny B (2011). Mechanisms of membrane curvature sensing. Annu Rev Biochem 80, 101–123.

Axe EL, Walker SA, Manifava M, Chandra P, Roderick HL, Habermann A, Griffiths G, Ktistakis NT (2008). Autophagosome formation from membrane compartments enriched in phosphatidylinositol 3-phosphate and dynamically connected to the endoplasmic reticulum. J Cell Biol 182, 685–701.

Bakula D, Muller AJ, Zuleger T, Takacs Z, Franz-Wachtel M, Thost AK, Brigger D, Tschan MP, Frickey T, Robenek H, *et al*. (2017). WIPI3 and WIPI4 beta-propellers are scaffolds for LKB1-AMPK-TSC signalling circuits in the control of autophagy. Nat Commun 8, 15637.

Baskaran S, Carlson L-A, Stjepanovic G, Young LN, Kim DJ, Grob P, Stanley RE, Nogales E, Hurley JH (2014). Architecture and dynamics of the autophagic phosphatidylinositol 3-kinase complex. Elife 3, e05115.

Behrends C, Sowa ME, Gygi SP, Harper JW (2010). Network organization of the human autophagy system. Nature 466, 68–76.

Blommaart EF, Krause U, Schellens JP, Vreeling-Sindelárová H, Meijer AJ (1997). The phosphatidylinositol 3-kinase inhibitors wortmannin and LY294002 inhibit autophagy in isolated rat hepatocytes. Eur J Biochem 243, 240–246.

Choi AMK, Ryter SW, Levine B (2013). Autophagy in human health and disease. N Engl J Med 368, 651–662.

Cong L, Ran FA, Cox D, Lin S, Barretto R, Habib N, Hsu PD, Wu X, Jiang W, Marraffini LA, Zhang F (2013). Multiplex genome engineering using CRISPR/Cas systems. Science 339, 819–823.

Dooley HC, Razi M, Polson HEJ, Girardin SE, Wilson MI, Tooze SA (2014). WIPI2 links LC3 conjugation with PI3P, autophagosome formation, and pathogen clearance by recruiting Atg12-5-16L1. Mol Cell 55, 238–252.

Drin G, Casella J-F, Gautier R, Boehmer T, Schwartz TU, Antonny B (2007). A general amphipathic alpha-helical motif for sensing membrane curvature. Nat Struct Mol Biol 14, 138–146.

Fan W, Nassiri A, Zhong Q (2011). Autophagosome targeting and membrane curvature sensing by Barkor/Atg14(L). Proc Natl Acad Sci USA 108, 7769–7774.

Fujita N, Itoh T, Omori H, Fukuda M, Noda T, Yoshimori T (2008). The Atg16L complex specifies the site of LC3 lipidation for membrane biogenesis in autophagy. Mol Biol Cell 19, 2092–2100.

Gammoh N, Florey O, Overholtzer M, Jiang X (2012). Interaction between FIP200 and ATG16L1 distinguishes ULK1 complex-dependent and -independent autophagy. Nat Struct Mol Biol 20, 144–149.

Gautier R, Douguet D, Antonny B, Drin G (2008). HELIQUEST: a web server to screen sequences with specific alpha-helical properties. Bioinformatics 24, 2101–2102.

Ge L, Baskaran S, Schekman R, Hurley JH (2014a). The protein-vesicle network of autophagy. Curr Opin Cell Biol 29C, 18–24.

Ge L, Melville D, Zhang M, Schekman R (2013). The ER-Golgi intermediate compartment is a key membrane source for the LC3 lipidation step of autophagosome biogenesis. Elife 2, e00947.

Ge L, Qi W, Wang L-J, Miao H-H, Qu Y-X, Li B-L, Song B-L (2011). Flotillins play an essential role in Niemann-Pick C1-like 1-mediated cholesterol uptake. Proc Natl Acad Sci USA 108, 551–556.

Ge L, Zhang M, Schekman R (2014b). Phosphatidylinositol 3-kinase and COPII generate LC3 lipidation vesicles from the ER-Golgi intermediate compartment. Elife 3.

Graef M, Friedman JR, Graham C, Babu M, Nunnari J (2013). ER exit sites are physical and functional core autophagosome biogenesis components. Mol Biol Cell 24, 2918–2931.

He S, Ni D, Ma B, Lee J-H, Zhang T, Ghozalli I, Pirooz SD, Zhao Z, Bharatham N, Li B, *et al*. (2013). PtdIns(3)P-bound UVRAG coordinates Golgi-ER retrograde and Atg9 transport by differential interactions with the ER tether and the beclin 1 complex. Nat Cell Biol 15, 1206–1219.

Hurley JH, Schulman BA (2014). Atomistic autophagy: the structures of cellular self-digestion. Cell 157, 300–311.

Itakura E, Kishi C, Inoue K, Mizushima N (2008). Beclin 1 forms two distinct phosphatidylinositol 3-kinase complexes with mammalian Atg14 and UVRAG. Mol Biol Cell 19, 5360–5372.

Itakura E, Mizushima N (2009). Atg14 and UVRAG: mutually exclusive subunits of mammalian Beclin 1-PI3K complexes. Autophagy 5, 534–536.

Itakura E, Mizushima N (2010). Characterization of autophagosome formation site by a hierarchical analysis of mammalian Atg proteins. Autophagy 6, 764–776.

Jinek M, East A, Cheng A, Lin S, Ma E, Doudna J (2013). RNA-programmed genome editing in human cells. Elife 2, e00471.

Kim J, Kim YC, Fang C, Russell RC, Kim JH, Fan W, Liu R, Zhong Q, Guan K-L (2013). Differential regulation of distinct Vps34 complexes by AMPK in nutrient stress and autophagy. Cell 152, 290–303.

Kim Y-M, Jung CH, Seo M, Kim EK, Park J-M, Bae SS, Kim D-H (2015). mTORC1 phosphorylates UVRAG to negatively regulate autophagosome and endosome maturation. Mol Cell 57, 207–218.

Kishi-Itakura C, Koyama-Honda I, Itakura E, Mizushima N (2014). Ultrastructural analysis of autophagosome organization using mammalian autophagy-deficient cells. J Cell Sci 127, 4089–4102.

Koyama-Honda I, Itakura E, Fujiwara TK, Mizushima N (2013). Temporal analysis of recruitment of mammalian ATG proteins to the autophagosome formation site. Autophagy 9, 1491–1499.

Lamb CA, Yoshimori T, Tooze SA (2013). The autophagosome: origins unknown, biogenesis complex. Nat Rev Mol Cell Biol 14, 759–774.

Liang C, Lee J-S, Inn K-S, Gack MU, Li Q, Roberts EA, Vergne I, Deretic V, Feng P, Akazawa C, Jung JU (2008). Beclin1-binding UVRAG targets the class C Vps complex to coordinate autophagosome maturation and endocytic trafficking. Nat Cell Biol 10, 776–787.

Ma X, Zhang S, He L, Rong Y, Brier LW, Sun Q, Liu R, Fan W, Chen S, Yue Z, *et al*. (2017). MTORC1-mediated NRBF2 phosphorylation functions as a switch for the class III PtdIns3K and autophagy. Autophagy 13, 592–607.

Matsunaga K, Morita E, Saitoh T, Akira S, Ktistakis NT, Izumi T, Noda T, Yoshimori T (2010). Autophagy requires endoplasmic reticulum targeting of the PI3-kinase complex via Atg14L. J Cell Biol 190, 511–521.

Matsunaga K, Saitoh T, Tabata K, Omori H, Satoh T, Kurotori N, Maejima I, Shirahama-Noda K, Ichimura T, Isobe T, *et al*. (2009). Two Beclin 1-binding proteins, Atg14L and Rubicon, reciprocally regulate autophagy at different stages. Nat Cell Biol 11, 385–396.

Mauthe M, Jacob A, Freiberger S, Hentschel K, Stierhof Y-D, Codogno P, Proikas-Cezanne T (2011). Resveratrol-mediated autophagy requires WIPI-1-regulated LC3 lipidation in the absence of induced phagophore formation. Autophagy 7, 1448–1461.

Mercer TJ, Gubas A, Tooze SA (2018). A molecular perspective of mammalian autophagosome biogenesis. J Biol Chem 293, 5386–5395.

Miller S, Tavshanjian B, Oleksy A, Perisic O, Houseman BT, Shokat KM, Williams RL (2010). Shaping development of autophagy inhibitors with the structure of the lipid kinase Vps34. Science 327, 1638–1642.

Mizushima N, Levine B, Cuervo AM, Klionsky DJ (2008). Autophagy fights disease through cellular self-digestion. Nature 451, 1069–1075.

Mizushima N, Yamamoto A, Hatano M, Kobayashi Y, Kabeya Y, Suzuki K, Tokuhisa T, Ohsumi Y, Yoshimori T (2001). Dissection of autophagosome formation using Apg5-deficient mouse embryonic stem cells. J Cell Biol 152, 657–668.

Nath S, Dancourt J, Shteyn V, Puente G, Fong WM, Nag S, Bewersdorf J, Yamamoto A, Antonny B, Melia TJ (2014). Lipidation of the LC3/GABARAP family of autophagy proteins relies on a membrane-curvature-sensing domain in Atg3. Nat Cell Biol 16, 415–424.

Nguyen N, Shteyn V, Melia TJ (2017). Sensing membrane curvature in macroautophagy. J Mol Biol 429, 457–472.

Nishimura T, Kaizuka T, Cadwell K, Sahani MH, Saitoh T, Akira S, Virgin HW, Mizushima N (2013). FIP200 regulates targeting of Atg16L1 to the isolation membrane. EMBO Rep 14, 284–291.

Obara K, Noda T, Niimi K, Ohsumi Y (2008). Transport of phosphatidylinositol 3-phosphate into the vacuole via autophagic membranes in Saccharomyces cerevisiae. Genes Cells 13, 537–547.

Pasquier B, El-Ahmad Y, Filoche-Romme B, Dureuil C, Fassy F, Abecassis P-Y, Mathieu M, Bertrand T, Benard T, Barrière C, *et al*. (2015). Discovery of (2S)-8-[(3R)-3-methylmorpholin-4-yl]-1-(3-methyl-2-oxobutyl)-2-(trifluoromethyl)-3,4-dihydro-2H-pyrimido[1,2-a]pyrimidin-6-one: a novel potent and selective inhibitor of Vps34 for the treatment of solid tumors. J Med Chem 58, 376–400.

Polson HEJ, de Lartigue J, Rigden DJ, Reedijk M, Urbé S, Clague MJ, Tooze SA (2010). Mammalian Atg18 (WIPI2) localizes to omegasome-anchored phagophores and positively regulates LC3 lipidation. Autophagy 6, 506–522.

Proikas-Cezanne T, Waddell S, Gaugel A, Frickey T, Lupas A, Nordheim A (2004). WIPI-1α (WIPI49), a member of the novel 7-bladed WIPI protein family, is aberrantly expressed in human cancer and is linked to starvation-induced autophagy. Oncogene 23, 9314–9325.

Ridley SH, Ktistakis N, Davidson K, Anderson KE, Manifava M, Ellson CD, Lipp P, Bootman M, Coadwell J, Nazarian A, *et al*. (2001). FENS-1 and

DFCP1 are FYVE domain-containing proteins with distinct functions in the endosomal and Golgi compartments. J Cell Sci 114, 3991–4000.
Ronan B, Flamand O, Vescovi L, Dureuil C, Durand L, Fassy F, Bachelot M-F, Lamberton A, Mathieu M, Bertrand T, *et al*. (2014). A highly potent and selective Vps34 inhibitor alters vesicle trafficking and autophagy. Nat Chem Biol 10, 1013–1019.
Rostislavleva K, Soler N, Ohashi Y, Zhang L, Pardon E, Burke JE, Masson GR, Johnson C, Steyaert J, Ktistakis NT, Williams RL (2015). Structure and flexibility of the endosomal Vps34 complex reveals the basis of its function on membranes. Science 350, aac7365.
Rubinsztein DC, Shpilka T, Elazar Z (2012). Mechanisms of autophagosome biogenesis. Curr Biol 22, R29–R34.
Sun Q, Fan W, Chen K, Ding X, Chen S, Zhong Q (2008). Identification of Barkor as a mammalian autophagy-specific factor for Beclin 1 and class III phosphatidylinositol 3-kinase. Proc Natl Acad Sci USA 105, 19211–19216.
Suzuki K, Akioka M, Kondo-Kakuta C, Yamamoto H, Ohsumi Y (2013). Fine mapping of autophagy-related proteins during autophagosome formation in Saccharomyces cerevisiae. J Cell Sci 126, 2534–2544.
Suzuki K, Kubota Y, Sekito T, Ohsumi Y (2007). Hierarchy of Atg proteins in pre-autophagosomal structure organization. Genes Cells 12, 209–218.
Takahashi Y, Coppola D, Matsushita N, Cualing HD, Sun M, Sato Y, Liang C, Jung JU, Cheng JQ, Mul JJ, *et al*. (2007). Bif-1 interacts with Beclin 1 through UVRAG and regulates autophagy and tumorigenesis. Nat Cell Biol 9, 1142–1151.
Takahashi Y, Meyerkord CL, Hori T, Runkle K, Fox TE, Kester M, Loughran TP, Wang H-G (2011). Bif-1 regulates Atg9 trafficking by mediating the fission of Golgi membranes during autophagy. Autophagy 7, 61–73.
Velikkakath AKG, Nishimura T, Oita E, Ishihara N, Mizushima N (2012). Mammalian Atg2 proteins are essential for autophagosome formation and important for regulation of size and distribution of lipid droplets. Mol Biol Cell 23, 896–909.
Wilz L, Fan W, Zhong Q (2011). Membrane curvature response in autophagy. Autophagy 7, 1249–1250.
Young LN, Cho K, Lawrence R, Zoncu R, Hurley JH (2016). Dynamics and architecture of the NRBF2-containing phosphatidylinositol 3-kinase complex I of autophagy. Proc Natl Acad Sci USA 113, 8224–8229.
Young LN, Hurley JH (2017). Mechanisms of autophagy initiation. Annu Rev Biochem.
Zhang M, Kenny SJ, Ge L, Xu K, Schekman R (2015). Translocation of interleukin-1β into a vesicle intermediate in autophagy-mediated secretion. Elife 4, e11205.
Zhong Y, Morris DH, Jin L, Patel MS, Karunakaran SK, Fu YJ, Matuszak EA, Weiss HL, Chait BT, Wang QJ (2014). Nrbf2 suppresses autophagy by modulating Atg14L-containing Beclin 1-Vps34 protein complex architecture and reducing intracellular phosphatidylinositol-3 phosphate levels. J Biol Chem 289, 26021–26037.
Zhong Y, Wang QJ, Li X, Yan Y, Backer JM, Chait BT, Heintz N, Yue Z (2009). Distinct regulation of autophagic activity by Atg14L and Rubicon associated with Beclin 1–phosphatidylinositol-3-kinase complex. Nat Cell Biol 11, 468–476.